Journal of Thermal Analysis and Calorimetry (2020) 139:3589–3602
https://doi.org/10.1007/s10973-019-08743-2

Preparation and performances characterization of HNIW/NTO-based high-energetic low vulnerable polymer-bonded explosive

Guanchao Lan[1] · Shaohua Jin[1] · Minglei Chen[2] · Jing Li[1] · Zhiyan Lu[2] · Na Wang[2] · Lijie Li[1]

Received: 16 January 2019 / Accepted: 21 August 2019 / Published online: 29 August 2019
© Akadémiai Kiadó, Budapest, Hungary 2019

Abstract
To satisfy the energy and security requirements of the explosives, it is necessary to develop high-energetic low vulnerable explosive. As the representatives of high-energetic explosives and low vulnerable explosives, hexanitrohexaazaisowurtzitane (HNIW) and 3-nitro-1,2,4-triazole-5-one (NTO) are used to research high-energetic low vulnerable polymer-bonded explosive (PBX) in this study. Based on the formulation of PAX-11 (94 mass% HNIW, 2.4 mass% CAB, 3.6 mass% BDNPA/F), some HNIW is replaced by NTO to reduce the vulnerability of the PBX during this work. Solution−water suspension method was used to prepare a series PBXs with different formulations. The explosion probability method, differential scanning calorimeter and accelerating rate calorimeter are used to evaluate the hazards of different PBX molding powders. And the thermal vulnerabilities, mechanical properties and energy levels of PBX columns are assessed by slow cook-off tests, tensile strengthes and detonation velocities, respectively. Moreover, finite element numerical simulations are adopted to study the transient temperature distributions, ignition time and ignition locations of the PBX columns during slow cook-off. The investigated results show that when the mass fraction of HNIW and NTO is 50% and 44%, respectively, the PBX passes the slow cook-off test and the detonation velocity reaches 8685 m s^{-1}. To balance the energy and vulnerability of the PBXs, we obtain a high-energetic low vulnerable PBX formulation (50 mass% HNIW, 44 mass% NTO, 2.4 mass% CAB, 3.6 mass% BDNPA/F, 0.5 mass% additional graphite) which can be used in the warhead of the high-explosive anti-tank cartridge.

Keywords HNIW · NTO · High energetic · Low vulnerable · PBX

Introduction

With the development of the technology, the defense capabilities of the military equipments are enhanced. Therefore, current interest has been focused on the development of high-energetic density materials (HEDMs) destroy the military equipments with great defense capabilities. Hexanitrohexaazaisowurtzitane (HNIW) possesses high energy, great density, strong detonation pressure and fast detonation velocity [1], which endows HNIW with broaden application prospects in HEDM field. Based on HNIW, many high-energetic explosives such as PAX-11, PAX-11(a), PAX-12 and PAX-29 have been prepared. However, the requirements of vulnerabilities and high energy are quite often contradictory to each other, resulting in greater hazards in the process of preparation, transportation and serving of the high-energetic explosives. Whenever the munitions with high vulnerability are subject to unplanned external stimuli, the munitions may detonate, which will produce huge damages. Therefore, for today's munitions, hazardous assessment against unplanned external mechanical and thermal stimuli have become an essential part of munitions development. Modern munitions are expected with the properties of low vulnerability to against unplanned external stimuli. This kind of munitions will flame or deflagrate rather than detonate when they are subject to strong unplanned external stimuli, which can minimize the probability of damage. Therefore, the development of low vulnerable munitions is necessary. One of the ideas for obtaining low vulnerable munitions is to replace some high vulnerable explosives by a certain

✉ Lijie Li
lilijie2003@bit.edu.cn

[1] School of Materials Science and Engineering, Beijing Institute of Technology, Beijing 100081, China

[2] Gansu Yin Guang Chemical Industry Group Co. Ltd, Baiyin 730900, China

amount of low vulnerability explosives such as 3-nitro-1,2,4-triazole-5-one (NTO) [2]. NTO, a highly potential insensitive high-performance explosive, has been well studied in many pressed and cast low vulnerable explosives compositions [2, 3]. Therefore, the high-energetic low vulnerable polymer-bonded explosive (PBX) could be obtained by mixing high-energetic explosive HNIW and low vulnerable explosive NTO together.

HNIW/NTO-based PBXs, which refer to a particle filled composite materials consisting of 90–95% mass of HNIW/NTO crystals held together by a small percentage polymer binder of 5–10% mass [4], possess the performances of HNIW and NTO. When the PBX suffers unplanned external stimuli, NTO can absorb and disperse the energy produced by the stimuli, which can decrease the formation probability of the hot spot on HNIW and reduce the hazardous risk. When the PBX is ignited by fuze, HNIW can produce high detonation pressure and fast detonation velocity which endows the PBX high damage efficiency. However, with the increase in NTO mass fraction, the vulnerability and energy of PBX are both decreased. Therefore, a suitable ratio between HNIW and NTO should be obtained to provide HNIW/NTO-based PBX with low vulnerability and high energy.

In this study, on the basis of PAX-11 (94 mass% HNIW, 2.4 mass% CAB, 3.6 mass% BDNPA/F), a certain amount of low vulnerable NTO is used as part replacements of some HNIW to decrease the vulnerability of the PBX with high energy during this work. A series of HNIW/NTO-based PBXs with different formulations are prepared to screen HNIW/NTO-based PBX formulation with high-energy low vulnerability. The analyses of geographies, mechanical sensitivities, thermal stabilities on the modeling powder and the studies of detonation velocity, mechanical properties and slow cook-off on PBXs columns are performed to evaluate the energy and security levels. Finite element numerical simulations, a good complementarity with experiment, are adopted to study the transient temperature distributions, ignition time and the ignition locations of the PBX columns during slow cook-off. The detailed experimental steps can be summarized in Fig. 1. Based on this study, we obtain a high-energetic low vulnerable PBX formulation which can be used in the warhead of the high-explosive anti-tank cartridge.

Experimental

Preparing of different PBXs

Solution–water suspension [5, 6] was used to prepare different HNIW/NTO-based modeling powders to study the coating effects, mechanical sensitivities and thermal stabilities. Based on the high-energetic explosive PAX-11 (94 mass% HNIW, 2.4 mass% CAB, 3.6 mass% BDNPA/F), several formulations were designed by replacing some HNIW with a certain amount of low vulnerable NTO to reduce the vulnerability of the PBX. The different formulations (by mass) of PBXs are displayed in Table 1. To further decrease the mechanical sensitivities and prevent static electricity, 0.5 mass% graphite is added to the surface of the PBXs. The modeling powders were further pressed to PBXs columns by hydraulic press to investigate the detonation velocities, mechanical properties and slow cook-off. Besides, the addition of graphite was benefit for the mold unloading after the press progress.

Geography studies of modeling powders

The coating effects and geographies of the binder system on HNIW and NTO were characterized by a TESCN MIRA3 XM SEM (Brno, Czech) instrument after gold sputtering coating under a 10^{-6} Pa vacuum. The macroscopic and microcosmic geographies of different modeling powders were obtained.

Mechanical sensitivity studies of modeling powders

The mechanical sensitivities of different modeling powders were measured after drying the samples for 6 h at 60 °C, applying the China National Military Standard GJB-772A [7]. During the tests, the ambient temperature was 21 °C and relative humidity was 67%. The impact sensitives were determined by fall hammer apparatus. The mass and vertical height of the hammer were 5 kg and 25 cm, respectively, and the samples mass was 30 ± 0.5 mg. The friction sensitivities were measured with the WM-1 pendular friction sensitivity apparatus using 90 pivot angle and 50 ± 0.5 mg of molding powders.

Thermal decomposition studies of modeling powders

A NETZSCH differential scanning calorimeter (DSC) 200 *F3* instrument was used to study the thermal decomposition properties of different modeling powders at ambient pressure with the aluminum crucible under dry, oxygen-free nitrogen atmosphere. The mass of each sample was about 1 mg, and the heating rates were 0.5, 1, 1.5, 2 °C min^{-1}, respectively.

Adiabatic thermal stability studies of modeling powders

A NETZSCH accelerating rate calorimeter (ARC) 254 instrument was adopted to determine the adiabatic thermal

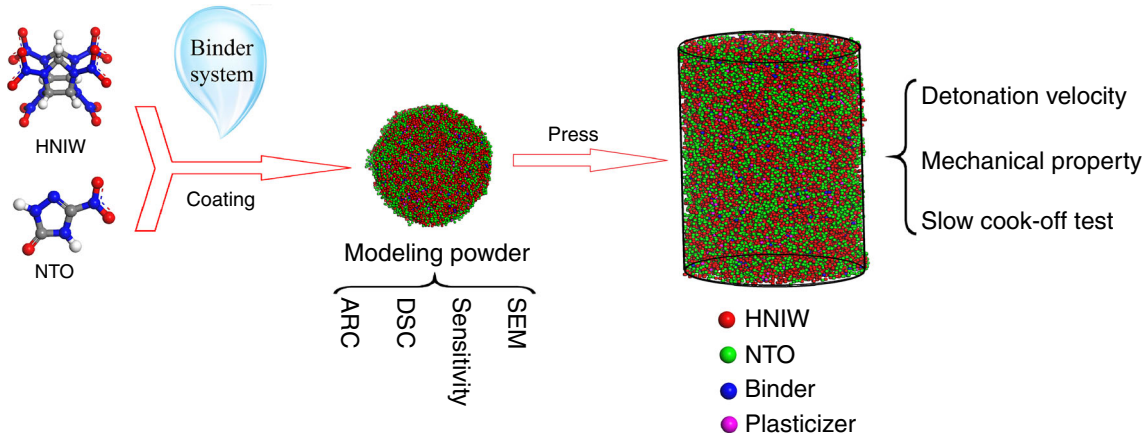

Fig. 1 Detailed experimental steps for obtaining HNIW/NTO-based high-energetic low vulnerable PBX

Table 1 Formulations (by mass) of different PBXs

	HNIW/mass%	NTO/mass%	CAB/mass%	BDNPA/F/mass%	G/mass%
PBX-1	54	40	2.4	3.6	0.5
PBX-2	50	44	2.4	3.6	0.5
PBX-3	47	47	2.4	3.6	0.5

stabilities of different modeling powders [8, 9]. 110 ± 1 mg samples were placed in a spherical Hastelloy C vessel with a volume of 10 mL and a mass of 21.5 g, and the standard 'heat-wait-search' procedure was used for these measurements with temperature increments of 5 °C. At each step, the system was kept adiabatic for a 'wait' period until thermal transients disappeared and then placed in 'search' mode, looking for an exotherm (self-heating rate ≥ 0.02 °C min^{-1}). ARC experiments were started at 50 °C, and the apparatus would repeat the heat-wait-seek model until the temperature reached 230 °C.

Detonation velocity studies of PBX columns

The detonation velocities of different PBXs were determined by applying the China National Military Standard GJB-772A [7]. The different modeling powders were pressed to three PBX columns with the diameter of 40 mm and the height of 40 mm, respectively. Then, the explosive columns were loaded (Fig. 2) to determine the detonation velocities. Because of the ion conductivity of the detonation wave front, the ionization pins and time measurement could test the travel time of the detonation wave front in the explosive column with a certain length. When the manganese pressure gauge was pressed by the detonation wave, its resistance increased with the increasing pressure. During the test, the room temperature was 26 °C and relative humidity was 68%.

Mechanical property studies of PBX columns

The tensile strengths of the columns were analyzed using Brazilian test [10–13] with an electromechanical universal testing machine (CMT4502, MTS Systems (China) Co., Ltd., Shanghai, China). A quasi-static radial compression load was imposed on the column with the loading rate of 0.5 mm min^{-1} to generate an axial tensile stress in the central area enough to damage the column. Then, the tensile strength, σ_t, could be calculated by the following equation [14]:

$$\sigma_t = \frac{2P}{\pi dh} \quad (1)$$

where P is the acting force, d is the diameter of column, and h is the thickness of the column.

The compression strengths of the columns were analyzed by an electromechanical universal testing machine (CMT4502, MTS Systems (China) Co., Ltd., Shanghai, China). A quasi-static axial compression load was imposed on the column with the loading rate of 0.5 mm min^{-1} until it was damaged. Then, the compression strength, σ_c, could be calculated by the following equation:

$$\sigma_c = \frac{4P}{\pi d^2} \quad (2)$$

where P is the acting force and d is the diameter of column.

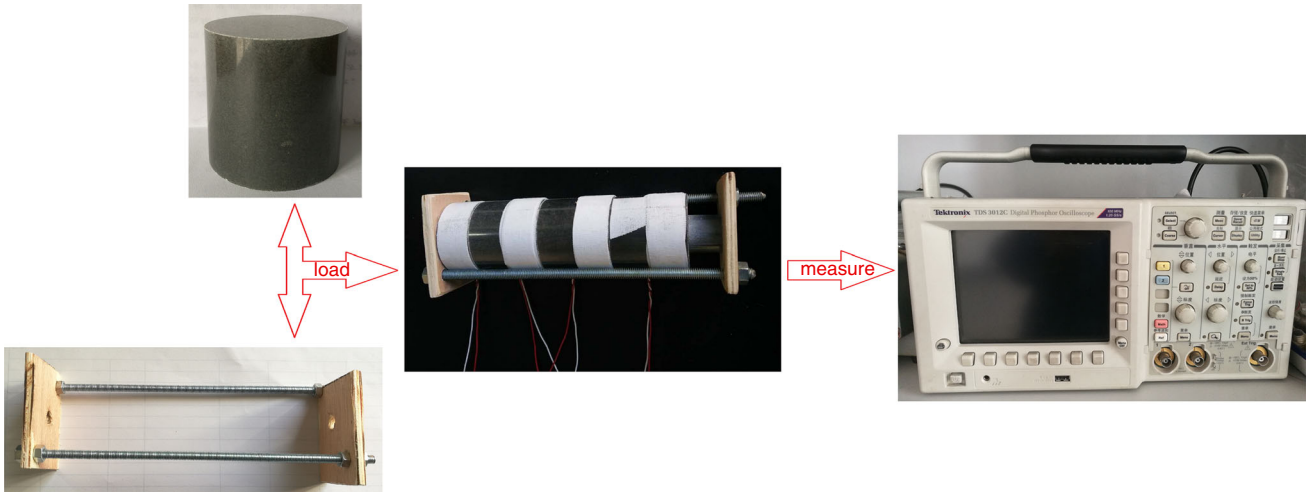

Fig. 2 Measurement of detonation velocities

Slow cook-off test studies of PBX columns

Slow cook-off is a test designed to simulate the hazard of a munition exposed to an engulfing liquid pool fire, such as ordnance suspended on an aircraft during a fire. In this study, a slow cook-off test setup was developed to study the response of different PBXs to the slow cook-off conditions. The experimental process of the slow cook-off test is shown in Fig. 3. The modeling powders were pressed into two columns with the diameter of 40 mm and the height of 40 mm, respectively. Then, the explosive columns were loaded in a slow cook-off bomb which consists of a hollow cylinder shell, two endcaps with screw threads, an electrical heat gun, a temperature control device and a thermocouple. The inner diameter, length and wall thickness of the cylinder bomb are 40 mm, 80 mm and 2.7 ± 0.05 mm, respectively. The wall thickness of the endcaps was 2.7 ± 0.05 mm as well. Then, cook-off the explosive columns with the heating rate of 1 °C min^{-1} until the PBXs were detonated or deflagrated.

Results and discussion

Geography analyses of modeling powders

The coating effects and geographies of modeling powders have significant influence on the performances of PBXs. In this study, the macroscopic and microcosmic geographies of the modeling powders with different formulations are analyzed by the SEM. As the difference between different formulations has little influence on the macroscopic and

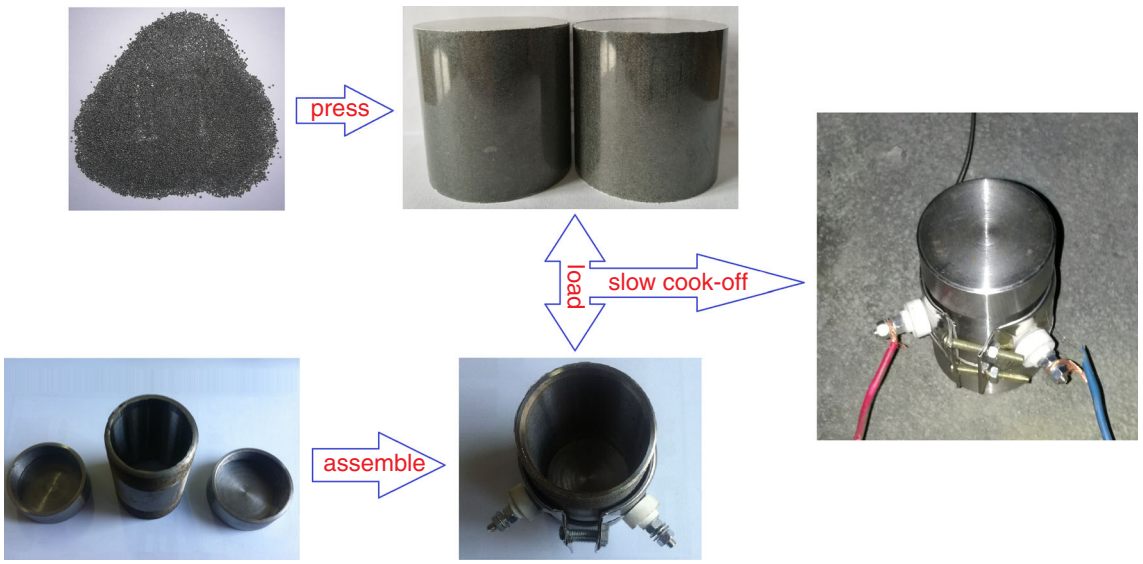

Fig. 3 Experimental process of the slow cook-off test

microcosmic geographies of molding powders, Fig. 4 only depicts the SEM results of modeling powder of PBX-2. Macroscopically, the particle size of modeling powders is homogeneous, and each modeling powder presents spherical shape. Microscopically, it can be deduced that the modeling powders are prepared by sticking every ε-HNIW and NTO crystal together with the help of the binder, and each explosive particle is wrapped well by the binder without explosive crystal surfaces exposed. As all explosive crystals are coated by the soft polymer binder, when modeling powders suffer the external mechanical stimulation, the binder can reduce the impact probability between explosive crystals, thus reducing the sensitivities. Besides, perfect coating effect is beneficial to the formability and mechanical property which are important for the PBXs.

Mechanical sensitivity analyses of molding powders

Hazards assessment against unplanned external mechanical stimuli is an essential part of munitions development. Mechanical sensitivity studies on modeling powders are the main method to evaluate the hazards of explosives against unplanned external mechanical stimuli. Explosives may be stimulated by external impact and friction during the production, transportation and application. Besides, if the mechanical sensitivities are poor, the modeling powders may detonate when pressing them into PBX columns, which brings tremendous security hazards. Therefore, it is necessary to study the impact and friction sensitivities of molding powders. The measured impact and friction sensitivities of different molding powders are summarized in Table 2.

Former practices have generally proved that the modeling powders would not detonate in the pressing process when the friction sensitivities are lower than 40%. As shown in Table 2, the friction sensitivities of three PBXs are all lower than 40%, which demonstrates that there is no security risk for pressing the modeling powders to PBX columns. Besides, it can be concluded from the measurement results that the mechanical sensitivities of the three modeling powders are sharply decreased compared with pure ε-HNIW, which illustrates that the security of these PBXs is enhanced. Therefore, the addition of NTO can decrease the hazards against unplanned external mechanical stimuli.

DSC analyses of modeling powders

The handling, storage and safety before deployment of explosives are key issues that confront the ammunition industry [15]. Precautions have to be taken not to cause premature detonations and fatal accidents by studying their thermal behaviors. DSC is one of the most widely used methods to research the thermal decomposition behaviors of PBXs. In this study, the DSC measurements of different modeling powders are implemented with the mass of each sample which is around 1 mg. The heating rates are 0.5, 1, 1.5 and 2 °C min^{-1}, because the decomposition mechanism is changed when the heating rate exceeds 2 °C min^{-1}. The measured results of every modeling powder under the heating rate of 1 °C min^{-1} are summarized in Fig. 5a.

It can be concluded from Fig. 5a that the orders of initial decomposition temperatures (T_o) and the peak temperature (T_p) of PBX-1, PBX-2 and PBX-3 are $T_{o(PBX\text{-}1)} > T_{o(PBX\text{-}2)} > T_{o(PBX\text{-}3)}$ and $T_{p(PBX\text{-}1)} < T_{p(PBX\text{-}2)} < T_{p(PBX\text{-}3)}$, respectively. PBX-1 possesses much shorter decomposition time than that of PBX-3, which means that NTO can expand the decomposition time range. Besides, the exothermic heat of the thermal decomposition is decreased with the increase in NTO mass fraction, demonstrating that the increasing NTO content has

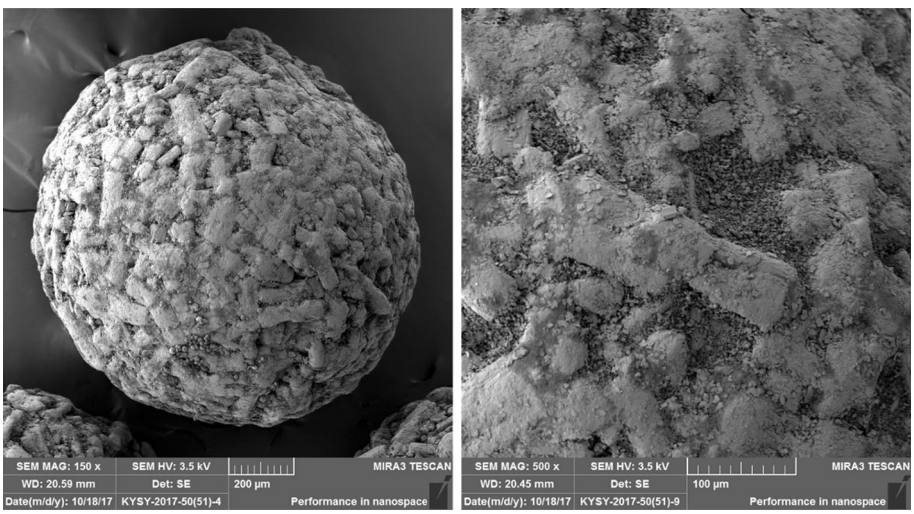

Fig. 4 Macroscopic and microcosmic geographies of PBX-2

Table 2 Measured impact and friction sensitivities of different molding powders

	Impact sensitivity/%	Friction sensitivity/%
ε-HNIW	100	100
PBX-1	8	4
PBX-2	16	20
PBX-3	28	16

negative influence on the detonation heat of PBXs. Therefore, the exothermic rate is decreased with the increasing NTO content, which most likely can be attributed to the expanded decomposition time ranges and the decreasing exothermic heat. The lower exothermic rate is benefit for the security.

The DSC measurements of different PBXs with the heating rate of 0.5, 1, 1.5 and 2 °C min^{-1} were performed to study the thermal decomposition kinetics. The measured results of PBX-2 are summarized in Fig. 5b. Based on the measurement results, the thermal decomposition kinetics are calculated by Kissinger and Ozawa methods [16, 17]. The calculated results of kinetic parameters are shown in Table 3.

The calculated thermo-kinetic parameters illustrate that with the increase in NTO, the activation energies are increased, which demonstrates that the thermal stabilities are enhanced. Therefore, the increasing NTO content is beneficial to decrease thermal hazards of PBXs against unplanned external thermal stimuli; meanwhile, the detonation heat is decreased as well.

ARC analyses of modeling powders

In real situations, energetic materials may suffer the adiabatic decomposition: ammunition with big size and low heat conductivity, energetic materials heated up by forced heating and showing a temperature increase in their center by heat accumulation (as in slow cook-off). From this point of view, the determination of self-heating has the intention to assess the hazards against thermal explosions. ARC can determine the self-heating of samples in an adiabatic environment. In this way, the decomposition process is controlled by sample rather than forced from an outside temperature program, which is similar with the real adiabatic decomposition. The ARC measurements were implemented to research the adiabatic thermal decomposition of different PBXs. In comparison with DSC, ARC determines the self-heating decomposition of the sample in an adiabatic environment with large sample amounts. The ARC determination results of different PBXs are summarized in Fig. 6a, and the variation of temperature (T), pressure (P), temperature change rate (dT/dt) and pressure change rate (dP/dt) with time (t) during the adiabatic decomposition process of PBX-2 is depicted in Fig. 6b.

Figure 6a illustrates that the initial adiabatic decomposition temperatures of PBX-1, PBX-2 and PBX-3 are 170.88 °C, 165.77 °C and 160.92 °C, respectively, which demonstrates that with the increase in NTO mass fraction, the initial adiabatic decomposition temperatures are decreased. In addition, the maximum adiabatic decomposition pressures of PBX-1, PBX-2 and PBX-3 are 1396.62 kPa, 1334.18 kPa and 1246.84 kPa, respectively, which illustrates that the increasing NTO content decreases the detonation pressure. The pressures begin to decrease after they reach the maximum, in that the gas produced by

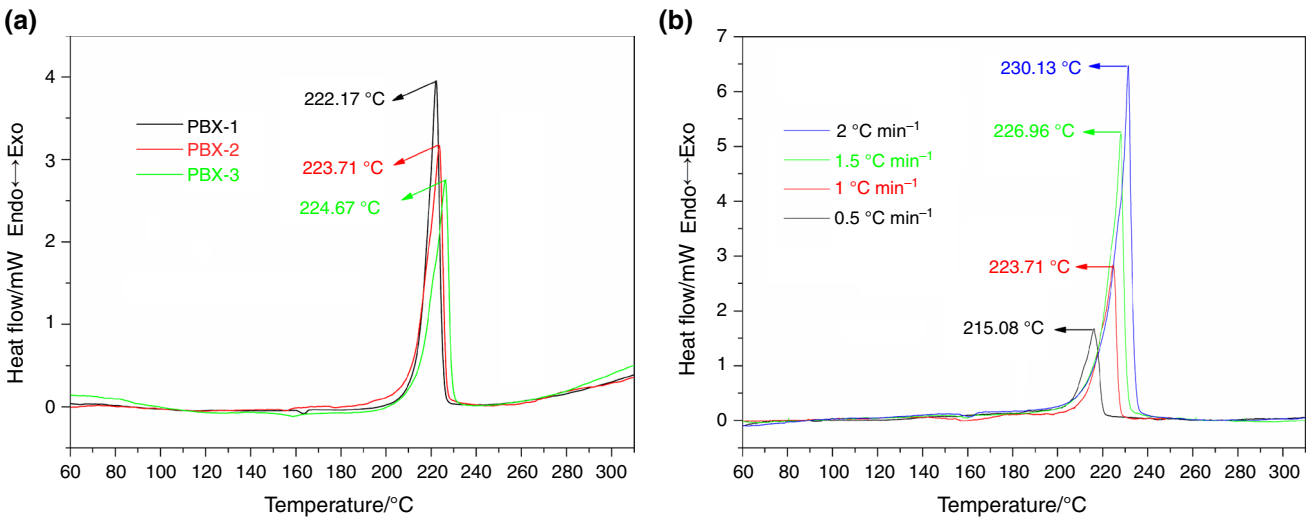

Fig. 5 **a** DSC measured results of different modeling powders under the heating rate of 1 °C min^{-1}; **b** the DSC measured results of PBX-2 under the heating rate of 0.5, 1, 1.5 and 2 °C min^{-1}, respectively

Table 3 Calculated thermo-kinetic parameters of different modeling powders

Sample	Kissinger			Ozawa	
	E_a/kJ mol^{-1}	A/s^{-1}	R^2	E_a/kJ mol^{-1}	R^2
PBX-1	178.676	1.155×10^{16}	0.991	177.714	0.991
PBX-2	179.424	1.269×10^{16}	0.991	178.435	0.992
PBX-3	180.164	1.390×10^{16}	0.991	179.158	0.991

the detonation of PBXs may react with each other. Moreover, when the temperatures and pressures of PBX-1, PBX-2 and PBX-3 reach (190.73 °C, 585.99 kPa), (192.91 °C, 621.64 kPa) and (198.97 °C, 638.63 kPa), respectively, the thermal decompositions are aggravated to thermal explosions due to the thermal accumulation. The pressures of the turn points increase with the increasing NTO content, which is benefit for PBX to pass the slow cook-off test, in that the pressure slowly increase before thermal explosions and the produced gas will attack the weakness location of the slow cook-off bomb. When the explosives are exploded, a large amount of gas is produced, resulting in that the pressure is sharply increased and the gas will attack everywhere of the slow cook-off bomb. Therefore, the higher the pressure produced before thermal explosions, the safer the munition is.

During the exothermal decomposition, the sample also heats up the measuring cell itself. This means that compared with a measurement without measuring cell, the self-heat rate is decreased by the measuring cell. So, it is necessary to correct the tested parameters to obtain the adiabatic decomposition parameters of the sample such as the adiabatic temperature rise, temperature rise rate and the time to maximum temperature rise rate. The above corrections could be processed using the thermal inertia factor (Φ), which is defined as follows [18–20]:

$$\Phi = 1 + \frac{m_M C_M}{m_s C_s} \tag{3}$$

where m_M, m_S, C_M and C_S are the measuring cell mass, sample mass, specific heat of measuring cell and specific heat of sample, respectively.

The corrected equations for some decomposition parameters are listed as follows [21, 22]:

$$\Delta T_{ad,s} = \Phi \Delta T_{ad} \tag{4}$$

$$T_{f,s} = \Phi \Delta T_{ad} + T_0 \tag{5}$$

$$\beta_{0,s} = \Phi \beta_0 \tag{6}$$

$$\beta_{m,s} = \Phi \beta_m \tag{7}$$

where $\Delta T_{ad,s}$ and ΔT_{ad} are the corrected and measured adiabatic temperature rise, respectively. $T_{f,s}$ is the corrected final decomposition temperature. T_0 is the measured initial decomposition temperature. $\beta_{0,s}$ and β_0 are the corrected and measured initial temperature rise rate, respectively. $\beta_{m,s}$ and β_m are the corrected and measured maximum temperature rise rate, respectively. The measured and corrected results are listed in Table 4.

Moreover, based on the ARC measurement results, the activation energies (E_a), pre-exponential factors (A) and mechanism functions of the adiabatic decomposition process of different modeling powders are calculated by the mechanism functions method [18, 23]. It can be seen from Fig. 6 that the decomposition of each modeling powder can be divided into two steps: slow thermal decomposition step and fast thermal explosion step. In this study, the E_a, A and mechanism functions of slow thermal decomposition step of each PBX are calculated. The 16 kinetic models and calculation results are depicted in Table 5.

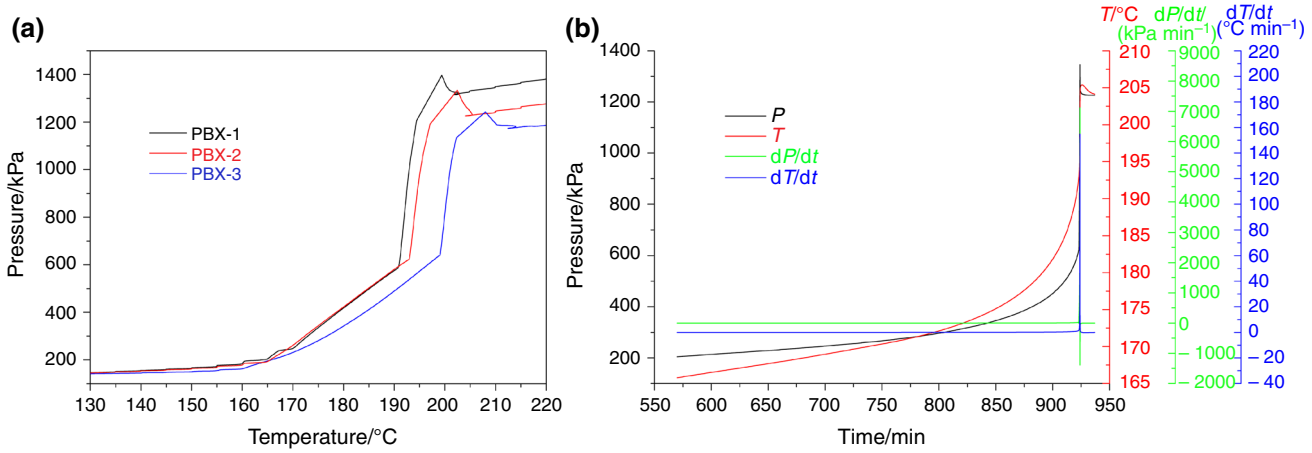

Fig. 6 **a** Measurement results of different modeling powders by ARC; **b** the variation of P, T, dP and dT versus t during the adiabatic decomposition process of PBX-2

The calculation results show that the adiabatic decomposition mechanism functions of PBX-1, PBX-2 and PBX-3 are $(1-\alpha)^2$. The obtained E_a, A and mechanism functions can be used to simulate the transient temperature distributions, ignition time and ignition locations of the PBX columns during slow cook-off. The E_a order of each PBX is $E_{a(PBX\text{-}1)} > E_{a(PBX\text{-}2)} > E_{a(PBX\text{-}3)}$. However, higher E_a does not mean higher thermal security. In order to judge the thermal securities of PBXs, SADT (self-accelerating decomposition temperature) is introduced.

SADT is defined as the lowest ambient air temperature at which a self-reactive substance or an organic peroxide of specified stability undergoes an exothermic reaction in a specified commercial package in a period of 7 days or less [24, 25]. SADT provides a good guide for evaluating the thermal hazards during the storing and transporting of hazardous materials [26, 27]. SADT of different modeling powders is calculated by the following equations [28, 29]:

$$\tau = \frac{MC_p}{US} \tag{8}$$

$$\mathrm{SADT} = T_{NR} - \frac{R(T_{NR}+273.15)^2}{E_a} \tag{9}$$

where τ is the time constant. M is the mass of packaged PBXs. C_p is the specific heat capacity of PBXs. U is the heat transfer coefficient of the package. S is the contact area of the system and environment. No return temperature, T_{NR}, is the temperature of a chemical substance above which the heat generated by a reaction exceeds the heat removal. When the temperature of a chemical system is above the T_{NR}, a thermal runaway reaction cannot be prevented from going to completion. T_{NR} can be obtained from the curve of the temperature at the time to maximum rate (T_{MR}) versus temperature by τ; E_a is the activation energy, and R is the gas constant.

In this study, 50 kg of different modeling powders is supposed to be stored in the wooden cylinder with the height of 60 cm, the diameter of 30 cm and U of 5 W m^{-2} $°C^{-1}$ [26]. As shown in Fig. 7, T_{NR} of different modeling powders is obtained, respectively. Subsequently, the SADTs are calculated, and the results are listed in Table 6.

The calculated SADT of PBX-3 (179.53 °C) is the highest, meaning that the thermal stability of PBX-3 is the best and the thermal hazard is the lowest. Former study [23] has reported that the SADTs of pure HNIW- and HNIW-based PBX (94 mass% HNIW, 2.5 mass% CAB, 2.5 mass% BDNPA/F, 1 mass% desensitizer) are around 142 °C and 157 °C, respectively. The SADTs obtained from this study are much higher than that of the reported, which illustrates that the addition of NTO can enhance the thermal securities and decrease the thermal hazards. Therefore, the increasing NTO content can decrease the hazards against unplanned external thermal stimuli, while the detonation pressure is decreased as well.

Detonation velocity analyses of PBX columns

Detonation velocity is a key property to evaluate the energy of the explosives. Generally, the energetic materials with higher detonation velocity have high energy. In order to evaluate the energy of the prepared PBXs, the modeling powders are pressed into PBXs columns, and then, the detonation velocities are determined. The average densities of explosive columns, calculated theory maximum detonation velocities (D_{TMD}) and measured average detonation velocities (D_e) are shown in Table 7.

As the explosive columns are pressed at room temperature rather than high temperature, the pressed densities are about 96.5% of the theory densities. The relative low densities result in the measured detonation velocities being lower than the theory maximum detonation velocities. Besides, the increasing NTO mass fraction decreases the detonation velocities of PBXs. The detonation velocities are still greater than 8500 m s^{-1}, when the mass fraction of NTO is less than 47%. On the basis of the service conditions, we can adjust the PBX formulation to satisfy the

Table 4 Measured and corrected thermal decomposition parameters of different modeling powders

Parameters	Measured results			Corrected results		
	PBX-1	PBX-2	PBX-3	PBX-1	PBX-2	PBX-3
C_p^a	0.958	0.937	0.929	–	–	–
Φ	–	–	–	87.59	88.33	89.08
T_0/ °C	170.88	165.77	160.92	–	–	–
T_f/ °C	201.83	204.13	211.06	2881.79	3554.11	4627.39
ΔT_{ad}/ °C	30.95	38.36	50.14	2710.91	3388.34	4466.47
β_0/ °C min^{-1}	0.0262	0.0247	0.027	2.29	2.18	2.41
β_m/ °C min^{-1}	166.00	154.93	129.06	14539.25	13683.86	11495.94

[a]C_p is the specific heat capacity of PBXs

Table 5 Activation energies (E_a), pre-exponential factors (A) and mechanism functions of different modeling powders

No.	$f(\alpha)$	PBX-1			PBX-2			PBX-3		
		R^2	E_a/kJ mol^{-1}	A/s^{-1}	R^2	E_a/kJ mol^{-1}	A/s^{-1}	R^2	E_a/kJ mol^{-1}	A/s^{-1}
1	$1/(2\alpha)$	0.7050	309.585	1.148×10^{31}	0.6950	463.760	4.850×10^{48}	0.6934	294.818	7.496×10^{28}
2	$2\alpha^{0.5}$	0.7050	− 154.792	1.402×10^{-23}	0.6950	− 231.880	2.845×10^{-32}	0.6934	− 147.409	1.442×10^{-22}
3	$1 - \alpha$	0. 9350	123.994	8.378×10^{9}	0.9686	113.970	4.854×10^{8}	0.9220	103.579	2.154×10^{7}
4	$(1 - \alpha)^2$	0. 9878	247.987	4.248×10^{24}	0.9886	227.941	1.185×10^{22}	0.9720	207.159	3.175×10^{19}
5	$2(1 - \alpha)^{3/2}$	0.8950	185.991	9.433×10^{16}	0.9286	170.956	1.199×10^{15}	0.8220	155.369	1.308×10^{13}
6	$[- \ln(1 - \alpha)]^{-1}$	0.7817	364.111	1.696×10^{37}	0.7600	516.697	4.023×10^{54}	0.7771	341.510	1.154×10^{34}
7	$3/2(1 - \alpha)^{2/3}[1 - (1 - \alpha)^{1/3}]^{-1}$	0.8452	426.958	1.069×10^{44}	0.8170	574.135	4.991×10^{60}	0.8438	393.873	3.634×10^{39}
8	$3/2(1 + \alpha)^{2/3}[(1 + \alpha)^{1/3} - 1]^{-1}$	0.6313	258.369	1.005×10^{24}	0.6289	402.208	3.057×10^{40}	0.6146	247.832	2.370×10^{22}
9	$3/2(1 - \alpha)^{2/3}[- \ln(1 - \alpha)]^{1/3}$	0.0007	2.623	5.538×10^{-5}	0.0387	− 58.262	5.511×10^{-12}	0.0129	− 10.257	1.553×10^{-6}
10	$4(1 - \alpha)[- \ln(1 - \alpha)]^{4/3}$	0.4372	− 149.090	6.497×10^{-23}	0.4964	− 273.552	4.021×10^{-37}	0.3800	− 152.553	3.614×10^{-23}
11	$3\alpha^{2/3}$	0.7050	− 206.390	1.115×10^{-29}	0.6950	− 309.173	2.693×10^{-41}	0.6934	− 196.545	2.599×10^{-28}
12	$3(1 - \alpha)^{2/3}$	0.8950	82.662	3.502×10^{4}	0.9286	75.980	5.576×10^{3}	0.8220	69.053	6.308×10^{2}
13	$2(1 - \alpha)^{1/2}$	0.8950	61.997	1.860×10^{2}	0.9286	56.985	49.110	0.8220	51.790	8.869
14	$3(1 - \alpha)[- \ln(1 - \alpha)]^{2/3}$	0.3742	− 118.747	2.745×10^{-19}	0.4498	− 230.494	4.693×10^{-32}	0.3100	− 124.094	8.402×10^{-20}
15	$2(1 - \alpha)[1 - \ln(1 - \alpha)]^{1/2}$	0.8394	85.227	1.034×10^{5}	0.8841	72.771	3.471×10^{3}	0.7419	69.404	1.020×10^{3}
16	$2/3[(1 - \alpha)^{-1/3} - 1]^{-1}$	0.8067	385.627	3.017×10^{39}	0.7817	536.145	3.871×10^{56}	0.8042	359.347	7.184×10^{35}

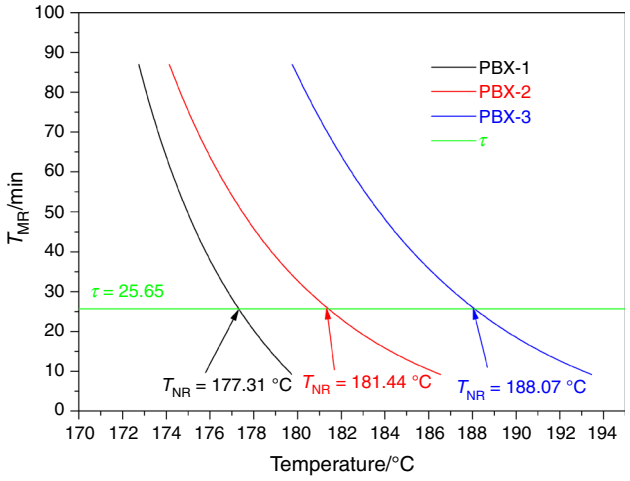

Fig. 7 Curves of T_{MR} versus temperature for different PBXs

Table 6 T_{NR} and SADT of different CAB/A3 binder systems

Samples	T_{NR}/ °C	SADT/ °C
PBX-1	177.31	170.51
PBX-2	181.44	173.90
PBX-3	188.07	179.53

security and energy demands. Therefore, the addition of NTO can decrease the detonation velocity of PBXs.

Mechanical property analyses of PBX columns

During the storage, transportation and application, PBXs with deficient mechanical properties might cause damages in the explosives, which can furthermore decrease the safety and detonation performance of the PBXs [28]. The damages in explosives can become the source of 'hot spots,' which might lead to ignitions under external accidental stimulation [29]. In addition, damages might affect the spread of detonation wave that decreases the power of the explosives. Therefore, the mechanical properties are important for the PBXs. In this study, the modeling powders are pressed into PBX columns with the diameter and height of 20 mm and 20 mm to measure the tensile strength and compressive strength. The measured results are displayed in Table 8.

As shown in Table 8, the tensile strengths of the PBX columns are slightly increased, and the compression strengths are greater than 14.32 MPa. It is deduced that the binding energy between NTO crystal surface and binder system might be higher than that between HNIW crystal surface and binder system. In general, the mechanical properties almost remain constant with the changing NTO content, which demonstrates that the mechanical properties mainly depend on the binder system [30, 32]. Therefore, the addition of NTO has little influence on the mechanical properties of PBXs.

Slow cook-off test analyses of PBX columns

Hazards assessment against unplanned external thermal stimuli is another essential part of munitions development. Slow cook-off studies on PBX columns are one of the main methods to evaluate the hazards of explosives against unplanned external thermal stimuli. Due to security requirements, low vulnerable munitions design against thermal stimuli like slow or fast cook-off has become a significant requirement for today's munitions [33]. In order to achieve low vulnerable munitions characteristics, the response of energetic material should immune to heating stimuli. Thermal initiation theory describes the ignition of detonation due to thermal effects from surrounding conditions and the heat generated inside the energetic material. Slow cook-off is an involuntary self-ignition phenomenon of an explosive in a cartridge often encountered in multiple sequential firings [34]. Slow cook-off can accurately evaluate thermal hazards of munitions. In this study, an efficient device has been used to study the slow cook-off of different PBX columns. The measurement results are summarized in Fig. 8.

Figure 8 shows that the cylinder shell of slow cook-off bomb is destroyed into fragments and no explosives left after the test of PBX-1, which illustrates that PBX-1 is detonated during the slow cook-off process. Therefore, PBX-1 does not pass the slow cook-off test and its thermal

Table 7 Average density of explosive columns, calculated theory maximum detonation velocities (D_{TMD}) and measured detonation velocities (D_e)

Samples	Density/g cm^{-3}	D^a_{TMD}/m s^{-1}	D_e/m s^{-1}
PBX-1	1.854	8779.19	8685
PBX-2	1.858	8740.66	8617
PBX-3	1.852	8711.84	8558

[a]The detonation velocities are calculated by Urazer method [30, 31]

Table 8 Measured tensile strength (σ_t) and compression strength (σ_c)

Samples	Density/(g·cm^{-3})	σ_t/MPa	σ_c/MPa
PBX-1	1.856	2.282	$> 14.32^a$
PBX-2	1.853	2.286	> 14.32
PBX-3	1.855	2.294	> 14.32

[a]The upper limit of the electromechanical universal testing machine was 4500 N, and the corresponding compression strength was 14.32 MPa

hazard properties are high. The endcaps of slow cook-off bombs are broken, while the cylinder shells are not deformed and many explosives are rushed out of the bombs, which demonstrates that PBX-2 and PBX-3 are flamed or deflagrated during the slow cook-off process. Therefore, PBX-2 and PBX-3 pass the slow cook-off test and their thermal hazard properties are low. The response temperatures of PBX-1, PBX-2 and PBX-3 are 218 °C, 198 °C and 191 °C, respectively, which demonstrates that higher response temperatures do not mean lower thermal hazards.

ARC measured results show that the decompositions of explosives can be divided into slow thermal decomposition step and thermal explosion step. Therefore, if an explosive can pass the slow cook-off test, the gas produced by the slow thermal decomposition step can burst the endcaps (weakest part) of the bomb and through the explosives out of the bomb to an open and low temperature environment. Otherwise, the explosives will detonate, resulting in the sharply increase in the pressure to destroy the bomb shell. ARC measured results also show that the slow thermal decompositions of PBXs will aggravate to thermal explosions due to thermal accumulation, when the temperatures and pressures of PBX-1, PBX-2 and PBX-3 reach to (190.73 °C, 585.99 kPa), (192.91 °C, 621.64 kPa) and (198.97 °C, 638.63 kPa), respectively. The pressure of PBX-1 (585.99 kPa) of the turn point is lower than that of PBX-2 (621.64 kPa) and PBX-3 (638.63 kPa), resulting in that the PBX-1 fails to burst the endcaps of the bomb before the detonation temperature. This phenomenon demonstrates that the maximum pressure of the slow cook-off bomb endcaps we used in this study can bear corresponding to the ARC pressure of 621.64 kPa. Therefore, based on the turn point pressure of decomposition–explosions transition, we can judge if a formulation can pass the slow cook-off test under the same test conditions.

Numerical simulation on the cook-off

One of the major problems resulting from an overheated explosion of a munition is the cook-off (self-ignition) phenomenon. Slow cook-off test can examine the vulnerability of an explosive, but it can hardly determine the transient temperature distribution ignition time and ignition location in the munitions which is significant for studying vulnerability. Finite element numerical simulation method is able to compensate for the shortcomings of experiment. Numerical simulation enables the designers to have an idea of when and where the energetic material ignites under certain adverse surrounding conditions [33]. In this study, based on the experiment results, ANSYS 15.0 academic finite element solver is used to simulate the temperature distribution, ignition time and ignition location of different PBX columns. The three-dimensional model of the system (PBX columns, endcaps and cylinder shell) and the created mesh are shown in Fig. 9.

Before starting the numerical analyses, all the boundary conditions are put into ANSYS program by user-defined function (UDF) according to experimental conditions. During the slow cook-off process, the PBX columns not only heat up by the external forced heating which has been defined in the boundary conditions of the UDF but also self-heat by the explosives released heat. As the slow cook-off can be regarded as an adiabatic decomposition process, the E_a, A and mechanism functions obtained by ARC analysis can be applied to describe the decomposition of PBX columns. Based on the PBX columns properties (released heat Q, E_a, A and mechanism functions of adiabatic decomposition), the cell zone conditions of PBX columns are put into ANSYS program by UDF. According to these conditions, ANSYS solves the problem using the proper time steps.

Taking PBX-1 as an example, Fig. 10 displays the evolution of transient temperature distribution from room

Fig. 8 Slow cook-off results of PBX-1, PBX-2 and PBX-3

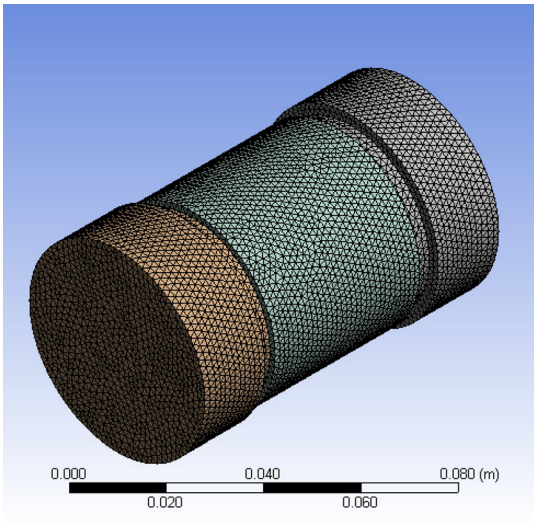

Fig. 9 3-D model of system and the created mesh

temperature to ignition temperature in the section plane along symmetry axis during slow cook-off.

As seen in Fig. 10a, the temperature distribution in the section plane shows that at the beginning of the slow cook-off, the temperature of the PBX columns close to the endcaps is lowest due to the low thermal conductivity of PBX columns. Then, the temperature of two endcaps is lowest due to convection between endcaps and air. At low temperature (< 170 °C), the maximum temperature occurs at the surface of the slow cook-off bomb, in that few PBXs are decomposed resulting in few heats accumulation. When the temperature is higher than 170 °C (Fig. 10b), due to the decomposition of PBX, the maximum temperature occurs at PBX columns. With the heat accumulation and heat conduction, the maximum temperature occurs around the center (Fig. 10c), which leads to the start of ignition. The experiment response time t_{res}, simulated ignition time t_{ign}, simulated ignition temperature T_{ign}, the experiment surface temperature $T_{surf\text{-}res}$ and simulated $T_{surf\text{-}ign}$ surface temperature outside the steel cook-off bomb at the response/ignition time of different PBX columns obtained from the simulation for the slow cook-off test are summarized in Table 9.

The study results illustrate that the simulated t_{ign} and $T_{surf\text{-}ign}$ of PBX-1 show good agreements with the experiment t_{res} and $T_{surf\text{-}res}$, which testifies the accuracy of simulation method. Therefore, the UDF we programmed is accurate and changing the Q, E_a, A and mechanism functions it can be used to simulate the slow cook-off of other system. However, the simulated t_{ign} and $T_{surf\text{-}ign}$ of PBX-2 and PBX-3 show relatively great deviations with the experimental results, in that before ignition, the produced gases break the endcaps of the slow cook-off bomb and through the PBX columns out of the bomb, resulting in that during experiment process, the determination is interrupted at the response temperature which is lower than ignition temperature. Therefore, the ignition situations can be obtained by simulation, which is a good complementation for the experiment.

Table 9 t_{res}, $T_{surf\text{-}res}$, t_{ign}, $T_{surf\text{-}ign}$ and T_{ign} of different PBX columns

		PBX-1	PBX-2	PBX-3
Experiment	t_{res}/s	8940	8340	8280
	$T_{surf\text{-}res}$/ °C	174	164	163
Simulation	t_{ign}/s	8784	8917	9128
	$T_{surf\text{-}ign}$/ °C	171.65	173.89	175.47
	T_{ign}/ °C	209.91	212.20	216.66

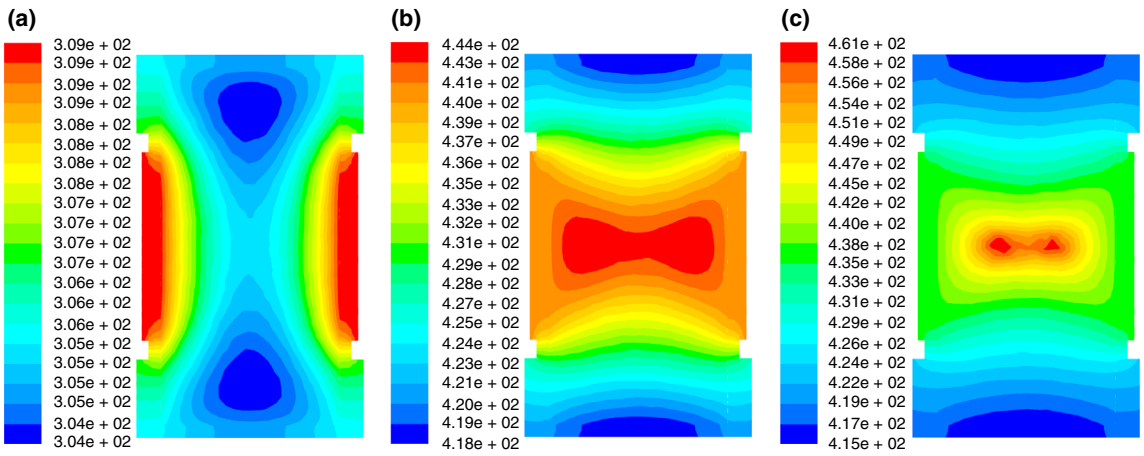

Fig. 10 Evolution of transient temperature distribution of PBX-3 during slow cook-off

Conclusions

HNIW/NTO-based PBXs with different formulations were prepared in this study. The geographies, mechanical sensitivities, thermal decompositions, detonation velocities, mechanical properties and slow cook-off tests were studied. The main conclusions can be summarized as follows:

(1) The addition of NTO will not significantly decrease the energy of the PBXs. Although the detonation velocities, detonation heats and detonation pressures of the PBXs are decreased with the increase in NTO, the measured detonation velocities are still greater than 8550 m s^{-1} even when the mass fraction of NTO is less than 47%.

(2) The addition of NTO will slightly affect the mechanical properties of the PBXs. With the increase in NTO, the tensile strengths of the PBX columns are slightly increased and the compression strengths are greater than 14.32 MPa. Besides, the mechanical properties mainly depend on the binder system and irrelevant to the NTO content.

(3) The addition of NTO will obviously increase the thermal securities and decrease the hazards of the PBXs. With the increase in NTO, the thermal hazards properties are decreased. The PBXs can pass the slow cook-off test when the mass fraction of NTO is more than 44%. The good complementarity between experiments and numerical simulations enables the designers to understand when and where the energetic material ignites under certain adverse surrounding conditions.

Above all, a HNIW/NTO-based high-energetic low vulnerable PBX formulation (50 mass% HNIW, 44 mass% NTO, 2.4 mass% CAB, 3.6 mass% BDNPA/F, 0.5 mass% graphite) is obtained. Owing to the properties of high energy and low vulnerability, it can be used in the warhead of the high-explosive anti-tank cartridge.

Acknowledgements This work was supported by the Fundamental Research Funds for the Central Universities.

References

1. Ou YX. Explosives. Beijing: Beijing Institute of Technology Press; 2014.
2. Becuwe A, Delclos A. Low sensitivity explosive compounds for low vulnerability warheads. Propell Explos Pyrot. 1993;18:1–10.
3. Mukundan T, Nair JK, Purandare GN, Talawar MB, Nath T, Asthana SN. Low vulnerable sheet explosive based on 3-nitro-1,2,4-triazol-5-one. J Propul Power. 2006;22:1348–52.
4. He GS, Yang ZJ, Zhou XY, Zhang JH, Pan LP, Liu SJ. Polymer bonded explosives (PBXs) with reduced thermal stress and sensitivity by thermal conductivity enhancement with graphene nanoplatelets. Compos Sci Technol. 2016;131:22–31.
5. Elbeih A, Pachman J, Zeman S, Trzcinski WA, Suceska M. Study of plastic explosives based on attractive cyclic nitramines: Part II. Detonation characteristics of explosives with polyfluorinated binders. Propell Explos Pyrot. 2013;38:238–43.
6. Niu H, Chen SS, Shu QH, Li LJ, Jin SH. Preparation, characterization and thermal risk evaluation of dihydroxylammonium 5, 5-bistetrazole-1, 1-diolate based polymer bonded explosive. J Hazard Mater. 2017;338:208–17.
7. GJB 772A, Explosive Test Method, Beijing, China, 1997.
8. Townsend DI, Tou JC. Thermal hazard evaluation by an accelerating rate calorimeter. Thermochim Acta. 1980;37:1–30.
9. Sridhar VP, Surianarayanan M, Sivapirakasam SP, Mandal AB. Adiabatic thermo kinetics and process safety of pyrotechnic mixtures. J Therm Anal Calorim. 2012;109:1387–95.
10. Palmer SJP, Field JE. The deformation and fracture of β-HMX. Proc R Soc A. 1982;383:399–407.
11. Palmer SJP, Field JE, Huntley JM. Deformation, strengths and strains to failure of polymer bonded explosives. Proc R Soc A. 1993;440:399–419.
12. Chen PW, Ding YS. Mechanical behavior and deformation and failure mechanisms of polymer bonded explosives. Chin J Energ Mater. 2000;8:161–4.
13. Berenbaum R, Brodie I. Measurement of the tensile strength of brittle materials. Br J Appl Phys. 1959;10:282–6.
14. Zhao YG, Fu H, Li YL, Chen R, Wen SG. Dynamic tensile mechanical properties of three types of PBX. China J Energy Mater. 2011;19:194–9.
15. Asante DO, Kim SH, Chae JS, Kim HS, Oh M. CFD cook-off simulation and thermal decomposition of confined high energetic material. Propell Explos Pyrot. 2015;40:699–705.
16. Bao F, Zhang GZ, Jin SH, Zhang CY, Niu H. Thermal decomposition and safety assessment of 3,30-dinitrimino-5,50-bis(1H-1,2,4-triazole) by DTA and ARC. J Therm Anal Calorim. 2018;132:805–11.
17. Bao F, Zhang GZ, Jin SH. Thermal decomposition behavior and thermal stability of DABT·2DMSO. J Therm Anal Calorim. 2018;131:3185–91.
18. Zhang GY, Jin SH, Li LJ, Li ZH, Shu QH, Wang DQ, Zhang B, Li YK. Evaluation of thermal hazards and thermo-kinetic parameters of 3-amino-4-amidoximinofurazan by ARC and TG. J Therm Anal Calorim. 2016;126:1223–30.
19. Li X, Chen SS, Zhang GY, Yu ZY, Li JX, Chen ML, Ma X, Xiang KL, Jin SH, Chen Y. Influence of energetic plasticizer bis(2,2-dinitropropyl)acetal/formal on properties of ε-CL-20 based pressed polymer-bonded explosives. Mater Express. 2017;7:216–22.
20. Zhang GY, Jin SH, Li LJ, Li YK, Wang DQ, Li W, Zhang T, Shu QH. Thermal hazard assessment of 4,10-dinitro-2,6,8,12-tetraoxa-4,10-diazaisowutrzitane (TEX) by accelerating rate calorimeter (ARC). J Therm Anal Calorim. 2016;126:467–71.
21. Zhang CY, Jin SH, Ji JW, Jing BC, Bao F, Zhang GY, Shu QH. Thermal hazard assessment of TNT and DNAN under adiabatic condition by using accelerating rate calorimeter (ARC). J Therm Anal Calorim. 2018;131:89–93.
22. Bao F, Zhang GZ, Jin SH, Zhang YP, Li LJ. Thermal decomposition and thermal stability of potassium 3,30-dinitrimino-5,50-bis(1H-1,2,4-triazole). J Therm Anal Calorim. 2018;133:1563–9.
23. Townsend DI, Tou JC. Thermal hazard evaluation by an accelerating rate calorimeter. Thermochim Acta. 1980;37:1–30.
24. Zou HM, Chen SS, Li X, Jin SH, Niu H, Wang F, Chao H, Fang T, Shu QH. Preparation, thermal investigation and detonation properties of ε-CL-20-based polymer-bonded explosives with high energy and reduced sensitivity. Mater Express. 2017;7:199–208.

25. Lv JY, Che LP, Chen WH, Gao HS, Peng MJ. Kinetic analysis and self-accelerating decomposition temperature (SADT) of dicumyl peroxide. Thermochim Acta. 2013;571:60–3.
26. Wang JF, Chen SS, Jin SH, Wang JY, Niu H, Zhang GY, Wang XJ, Wang DX. Size-dependent effect on thermal decomposition and hazard assessment of TKX-50 under adiabatic condition. Propell Explos Pyrot. 2018;43:488–95.
27. Fisher HG, Goetz DD. Determination of self-accelerating decomposition temperatures using the accelerating rate calorimeter. J Loss Prev Process Ind. 1991;4:305–16.
28. Liu JH, Yang ZJ, Liu SJ, Zhang JH, Liu YG. Effects of fluoropolymer binders on the mechanical properties of TATB-based PBX. Propell Explos Pyrot. 2018;43:664–70.
29. Mulford RN, Swift D. Sensitivity of PBX-9502 after ratchet growth. AIP Conf Proc. 2012;1426:311–4.
30. Sun YB, Hui JM, Cao XM. Military use blended explosives. Beijing: Weapon Industry Press; 1995.
31. Jin SH, Song QC. Explosive theory. Xian: Northwestern Polytechnical University Press; 2010.
32. Hoffman DM. Dynamic mechanical signatures of Viton A and plastic bonded explosives based on this polymer. Polym Eng Sci. 2003;43:139–56.
33. Aydemir E, Ulas A. A numerical study on the thermal initiation of a confined explosive in 2-D geometry. J Hazard Mater. 2011;186:396–400.
34. Halil I, Fatih G. Cook-off analysis of a propellant in a 7.62 mm barrel by experimental and numerical methods. Appl Therm Eng. 2017;112:484–96.

Publisher's Note Springer Nature remains neutral with regard to jurisdictional claims in published maps and institutional affiliations.